International Journal of Automotive Technology, Vol. 18, No. 6, pp. 993−1006 (2017)
DOI 10.1007/s12239−017−0097−2

pISSN 1229−9138/ eISSN 1976−3832

VEHICLE STABILITY CONTROL BASED ON DRIVER'S EMERGENCY ALIGNMENT INTENTION RECOGNITION

Xia Xin[1, 2)], Xiong Lu[1, 2)*], Hou Yuye[1, 2)], Teng Guowen[1, 2)] and Yu Zhuoping[1, 2)]

[1)]School of Automotive Studies, Tongji University, Shanghai 201804, China
[2)]National "2011" Collaborative Innovation Center, Tongji University, Shanghai 201804, China

(Received 23 December 2016; Revised 25 March 2017; Accepted 10 May 2017)

ABSTRACT−In this work, the reference model modification strategy for vehicle stability control based on driver's intention recognition under emergent obstacle avoidance situation was proposed. First the conflicts between the driver's emergency alignment (EA) intention and vehicle response characteristics were analyzed in critical emergent obstacle avoidance situation. Second combining steering wheel angle and its speed, the driver's EA intention was recognized. The reference model modification strategy based on steering operation index (SOI) was presented. Then a LQR model following controller with tire cornering stiffness adaption was used to generate direct yaw moment for tracking modified reference yaw rate and reference sideslip angle. Finally based on the four-in-wheel-motor-drive (FIWMD) electric vehicles (EV), double lane change and slalom tests were conducted to compare the results using modified reference model with the results using normal reference model. The experimental tests have proved the effectiveness of the reference model modification strategy based on driver's intention recognition.

KEY WORDS : Emergent obstacle avoidance, Driver's EA intention recognition, Reference model modification, Stability control

NOMENCLATURE

γ_d : desired yaw rate, rad/s
γ_r : reference yaw rate
γ_{mr} : modified reference yaw rate
m : vehicle mass,
C_f : front equivalent cornering stiffness
C_r : rear equivalent cornering stiffness
l : wheel base
l_f : distances from the front axis to COG
l_r : distances from the rear axis to COG
v_x : longitudinal velocity
μ : maximum road friction coefficient
δ_f : steering angle of front wheel
i_f : steering ratio
g : acceleration of gravity
β : sideslip angle
$\dot{\beta}$: derivative of sideslip angle
a_y : lateral acceleration
γ : yaw rate
s : Laplace operator
J_z : vehicle yaw moment of inertia
δ_n : nominal steering wheel angle
δ_{sw} : actual steering wheel angle
$\dot{\delta}_{sw}$: derivative of actual steering wheel angle
δ_{lower_limit} : lower limit of steering wheel angle
$\dot{\delta}_{sw\_lower\ limit}$: derivative of lower limit of steering wheel angle speed
T_{act} : time threshold before activating the recognition module
T_{exit} : time threshold before turning off the recognition module
$\beta_{lower\ limit}$: lower limit of reference sideslip angel
$\beta_{upper\ limit}$: upper limit of reference sideslip angel
β_r : reference sideslip angel
M_z : direct yaw moment
y : observed vector
ϕ : measured vector
θ : estimated vector
λ_1 : forgetting factor of front axle
λ_2 : forgetting factor of rear axle
Q : weight matrix of control tracking error
R : weight matrix of control input
B : effectiveness matrix
b_f : front wheel base
b_r : rear wheel base
u_c : control input

*Corresponding author. e-mail: xiong_lu@tongji.edu.cn
*This paper was modified from the original paper presented in FISITA World Automotive Congress 2016, and recommended by the Scientific & Technical Committee for journal publication.

1. INTRODUCTION

It is well known that safety has always been a main topic in

the developing process of vehicle. Currently electronic stability control (ESC) is widely used as a useful vehicle stability control system (Erke, 2008). In most situations, the driver only needs to steer regularly in a quasi-static condition to drive the vehicle under his intention. The yaw rate response and sideslip angle response could follow the driver's steering intention well and there won't be unnecessary and excessive steering operation. However under critical emergent obstacle avoidance situation at high velocity, normal inexperienced drivers lacking of awareness of the vehicle nonlinear characteristic and response lag usually tend to automatically steer too much and then worsen the situation (Zanten, 2000; Anton *et al*., 1998). At this time if ESC intervenes to force the vehicle follow the desired yaw rate and sideslip angle which are proportional to the excessive steering angle based on the conventional reference model, it will aggravate the nonlinearity and the vehicle may lose its stability. Based on the above, this paper focuses on recognizing the driver's emergency steering intention and modifying the reference model according to the steering intention to impel the vehicle to follow the driver's intention better and improve the driver-vehicle-road safety under critical emergent obstacle avoidance situation at high velocity through dynamics control.

According to the state of the art, the existing vehicle stability control systems most directly use the steering wheel angle to reflect the driver's steering intention which means the desired yaw rate and sideslip angle are calculated only on the basis of the steering angle and then use a model following control (MFC) method to keep the vehicle follow the reference model (Peng and Hori, 2006). The two degree of freedom linear vehicle model was used to described the vehicle lateral dynamics and the yaw rate and sideslip angle response to steering angle were used as the desired reference value (Abe, 1999; Tahami *et al*., 2002; Geng *et al*., 2009; Li *et al*., 2015; Alipour and Sabahi, 2015; Emirler *et al*., 2015; Yu *et al*., 2015; Chen *et al*., 2016; Shen *et al*., 2016). The second order single track bicycle model system was simplified as first order system to calculate the desired reference value (Yang *et al*., 2009). The dynamic process of bicycle model was ignored and the desired yaw rate was in proportion to steering angle (Ding and Taheri, 2010). Sideslip angle was used to regulate and restrain the desired yaw rate calculated from the bicycle model to coordinate the handling and stability performance (Teng *et al*., 2015). The sideslip angle was set zero to fulfill the stability requirement but the yaw rate gain was weaken (Shino and Nagai, 2001). The reference models above have also considered the constraints from road friction coefficient. In addition, in critical emergent obstacle avoidance situation at high velocity, normal drivers may steer fast in order to avoid obstacle. In other word, the driver's urgency of steering could be reflected by the steering velocity information exactly. Those kinds of reference model ignored the steering velocity and cannot recognize and reflect the urgent steering behaviors.

In recent years, some researchers have involved the driver's intention into the vehicle dynamics control. The Hidden Markov Model was used to recognize driver's steering intention and the desired yaw rates were switched by a weighting coefficient (Raksincharoensak *et al*., 2009). The steering wheel angle and its speed were used to analyze the steering demand and steering intention based on the steering behavior index (Lee *et al*., 2014). In addition, according to the steering angle direction, steering velocity direction and yaw rate direction, the control strategy was designed through logical judgment (Yu *et al*., 2006). The derivative of yaw rate deviation was used to reflect the vehicle response speed to the driver's intention. The working condition was divided into multiple cases to determine which wheel needed to brake (Gan *et al*., 2014). Those two control strategy only track the yaw rate and restrain sideslip angle indirectly. The stability of the control methods needed further research. The frequent switch in different cases would interfere with the driver's operation and intensify the panic. In our previous research in this area, we divided the regular steering and EA in two situations. And the yaw moment gain varies jumping from 0 to 1 (Xiong *et al*., 2016). The intervention feeling was too strong for the driver which would also intensify the panic. The main contribution of this paper is that we modified the reference model further instead of switching the direct yaw moment from the normal direct yaw moment and emergent yaw moment roughly and proposed this continues equivalent-gain-schedule control method compared to our previous work.

In this paper, the reference model modification strategy based on driver's intention recognition was put forward and used in the stability control. First, the vehicle response lag to the steering operation was analyzed. Second, the driver's EA intention recognition method was proposed. The reference model modification strategy was presented based on the SOI. Then, a LQR motion tracking controller with cornering stiffness adaption was used to keep the vehicle following the reference model. Finally, many double lane change and slalom experiments were conducted on a FIWMD EV based on its merit in dynamics control (Shino and Nagao, 2003; Yu *et al*., 2013; Li *et al*., 2013b). The effectiveness of the modified reference model has been validated. The driver's EA steering intention has been realized better and the vehicle stability especially under EA situation at high velocity situation has been improved (Xia *et al.*, 2016).

The remainder of this paper is organized as follows: The reference model, yaw rate response and sideslip angle response of the vehicle are analyzed in Section 2. Section 3 presents the reference model modification strategy. The ESC controller is introduced in Section 4. Section 5 shows the experimental results in real tests. In the end this research and introduction for future work are summarized in the Section 6.

2. ESC REFERENCE MODEL ANALYSIS

2.1. Conventional Reference Model

Considering the road friction constraint, the existing ESC systems usually take Equations (1) and (2) to calculate reference yaw rate (Rajamani, 2005).

$$\gamma_d = \frac{v_x / l}{1 + \frac{m}{l^2}\left(\frac{l_f}{C_r} - \frac{l_r}{C_f}\right) v_x^2} \cdot \delta_f \tag{1}$$

$$\gamma_r = \begin{cases} \gamma_d, & |\gamma_d| \le \dfrac{0.85\mu g}{v_x} \\ \dfrac{0.85\mu g}{v_x} \cdot \mathrm{sgn}(\gamma_d), & |\gamma_d| > \dfrac{0.85\mu g}{v_x} \end{cases} \tag{2}$$

Usually there are two methods to choose the reference sideslip angle: 1) The sideslip angle is set zero to fulfill the stability requirement but the yaw rate gain will be weaken which will increase the driver's steering burden and even make the vehicle hard to steer in critical situation (Shino and Nagai, 2001); 2) The sideslip angle is limited under certain upper bound according to the road friction condition through controlling yaw rate directly (Yang, 2011). Figure 1 shows the flow diagram.

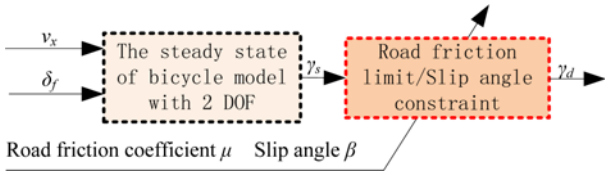

Figure 1. Conventional reference model diagram.

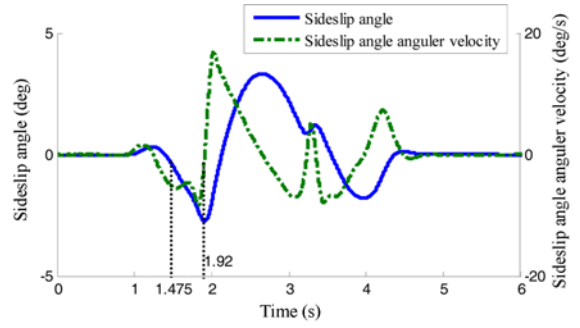

(a) Sideslip angle

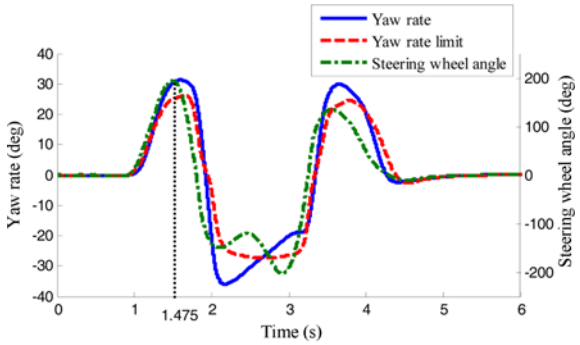

(b) Yaw rate and steering wheel angle

Figure 2. Simulation results of double lane change maneuver.

Then based on critical emergent obstacle avoidance situation at high velocity especially the emergency alignment situation, the conflicts between sideslip angle response and yaw rate response and the drive's intention are analyzed to show the drawbacks of the existing reference model.

2.2. Sideslip Angle Response in Emergent Obstacle Avoidance Situation

First the sideslip angle response in emergent obstacle avoidance situation is simulated in Carsim software. The FIWMD EV model is built with parameters in Tables 1 and 2 (Xiong *et al*., 2014). In order to simulate the emergency steering behavior, the double lane change maneuver is considered. The velocity is 60 km/h and maximum road friction coefficient is 0.8. The simulation results are shown in Figure 2.

As shown in Figure 2, take the first lane change for example, steering wheel angle reaches peak value at 1.475 s, yaw rate reaches peak value at 1.61 s, and sideslip angle reaches peak value at 1.92 s. The yaw rate response lags behind the steering angle and the sideslip angle response lags behind the yaw rate.

According to the 2DOF vehicle dynamics model, Equation (3) can be obtained.

$$\dot{\beta} = \frac{a_y}{v_x} - \gamma \tag{3}$$

We call the first item a_y/v_x on the right side of Equation (3) the yaw rate limit.

In the steering wheel angle increase and alignment process (t < 1.92 s), the sideslip angle grows to its peak value. This whole process can be divided into two parts. The first part is associated with the increasing steering wheel angle until t = 1.475 s. The sideslip angle increases to a certain negative value. The increase of sideslip angle in this part is necessary because the driver wants to steer fast. The second part is associated with EA process (t = 1.475 s ~ 1.92 s). The aligning of steering wheel denotes the driver wants the vehicle to travel back towards the opposite side or to travel straight which means both sideslip angle and yaw rate should decrease at this moment immediately but the sideslip angle still increase until the yaw rate limit is equal to the yaw rate. In this EA process, the lateral velocity and lateral displacement increase simultaneously because of the increasing sideslip angle. Apparently, the driver's EA intention conflicts with the real sideslip angle response because of its continuous increase when the steering wheel starts to align. And this conflict may cause the excessive steering of the driver which then may make

the vehicle lose its stability.

In order to explain this phenomenon, based on the linear 2DOF single track vehicle model, we can obtain the transfer function from steering angle to sideslip angle as Equation (4) (Abe, 2009).

$$\frac{\beta(s)}{\delta_f(s)} = \left.\frac{\beta}{\delta_f}\right|_s \cdot \frac{1+Ts}{1+\frac{2K_1}{H}s+\frac{1}{H}s^2} \tag{4}$$

Where

$$K_1 = -\frac{J_z(C_f+C_r)+m(C_f l_f^2+C_r l_r^2)}{2J_z m v_x},$$

$$T = -\frac{J_z v_x}{C_r l_r l + l_f m v_x^2}, \quad H = \frac{C_f C_r l^2 + m v_x^2 (C_f l_f - C_r l_r)}{J_z m v_x^2}.$$

The steady gain is

$$\left.\frac{\beta}{\delta_f}\right|_s = \frac{C_f(C_r l_r l + l_f m v_x^2)}{l^2 C_f C_r + (C_f l_f - C_r l_r) m v_x^2} \tag{5}$$

From Equation (4), the zero point can be derived as Equation (6).

$$s = -\frac{1}{T} = \frac{C_r l_r l + l_f m v_x^2}{J_z v_x} \tag{6}$$

In the emergent obstacle avoidance situation, the tire cornering stiffness would decrease with the increase of the slip angle. According to Equation (6), on the one hand, the zero point would become positive when the cornering stiffness decreases to a certain value at a certain velocity. The system denoted by Equation (4) becomes a non-minimum phase system and the sideslip angle delay would increase more; on the other hand, even the tire slip angle is small, the system denoted by Equation (4) also becomes non-minimum phase system with the increase of the velocity. Figure 3 shows the relationship between the sideslip angle phase lag and rear axle cornering stiffness. The frequency of steering angle input is 0.7 Hz and the velocity is 60 km/h to simulate the emergent obstacle avoidance situation. The phase lag would increase with the decrease of the cornering stiffness.

Therefore when the driver steers emergently at high velocity to avoid obstacle, in the time domain, the sideslip angle lags seriously behind the steering angle. In the t = 1.475 ~ 1.92 process, the tire slip angle would increase

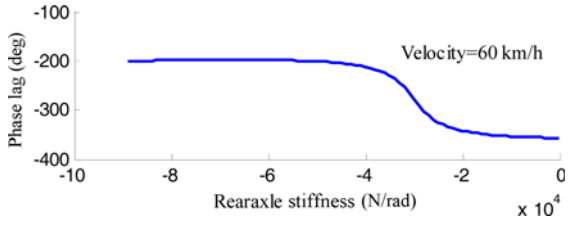

Figure 3. Sideslip angle phase lag about rear axle stiffness.

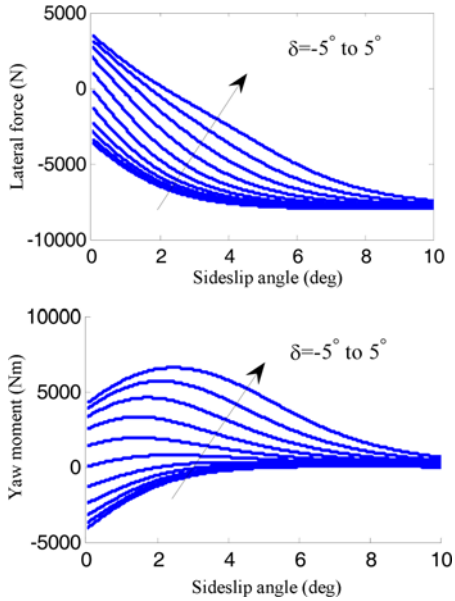

Figure 4. β-lateral force and yaw moment diagram.

further, the vehicle slip angle would also increase, and the lateral acceleration would increase which will intensify the tire saturation. As a result, the cornering stiffness decreases and the sideslip angle lag increases in return. The conflicts between the vehicle state response and the driver's intention exist in the whole EA process. Thus it is urgent to recognize driver's EA intention and modify the reference model to create a larger direct yaw moment to help driver emergently align.

In addition, referring to the β method (Shibahata *et al.*, 1993), we obtain the relationship between lateral force and yaw moment and sideslip angle depicted in Figure 4 on road condition where $\mu = 0.8$. δ caused by steering angle is the difference of slip angle of front and rear axle. On different road, the curves in Figure 4 differ a lot. The lateral force would vary with sideslip angle when the slip angle is small and come to the saturate value when the sideslip angle increases to a certain value. At small sideslip angle, the yaw moment can easily be changed by steering angle. When the sideslip angle increases to a certain large value, the yaw moment decreases sharply to small value with increase of the sideslip angle which shows that the lateral forces cannot provide the yaw moment and the change of steering angle has little influence on the yaw moment. In this sense, when the sideslip angle is large at EA situation, large longitudinal tire forces are needed to help the driver steering.

The conventional researches use MFC methods to keep the vehicle following a normal reference model which lacks of considering the large response lag and the driver's intention. Few existing researches focus on this special EA situation. Based on the analysis above, in EA situation, a larger yaw moment is needed than other situation because of the conflicts and vehicle response characteristic. In this

paper, when the EA situation is recognized, the reference yaw rate would be decreased to create a large yaw moment to realize gain-scheduling indirectly.

2.3. Yaw Rate Response in Emergent Obstacle Avoidance Situation

In emergent obstacle avoidance situation especially in EA situation, from the yaw rate point, the reference yaw rate in conventional reference model such as Equations (1) and (2) also has some drawbacks. Normally the driver's yaw requirement can be interpreted by Equation (1) without considering the road limit. The reference yaw rate is obtained by Equation (2). For the sake of convenience, here we exert a single sine wave steering wheel angle to the vehicle to simulate the emergent obstacle avoidance situation. The simulation results are shown in Figure 5.

As Figure 5 shows, at the first stage, before the reference yaw rate gets to road limit (Equation (2)), the reference model can reflect the driver's intention well. Then with the steering wheel angle increasing further until its maximum value in normal region and region I parts and decreasing to the road limit in region II part, the reference yaw rate remains constant and the driver's intention cannot be satisfied. In region I, the driver's intention cannot be satisfied because the actual yaw rate cannot follow the driver's yaw rate requirement since the road limit. In region II, the driver emergently aligns which means the driver wants the yaw rate to decrease fast to the opposite direction. In this stage, we can recognize that EA intention, and reduce the reference yaw rate to create a larger yaw rate tracking error for the MFC controller which will produce a larger direct yaw moment to help driver emergently align than conventional reference model. That is to say, the driver's intention could be satisfied better than the conventional reference model.

The steering wheel angle and its speed interpret the driver's intention directly. Therefore we involve steering wheel angle information to analyze the driver's intention. We introduce a new variable called nominal steering wheel angle δ_n defined by Equation (7).

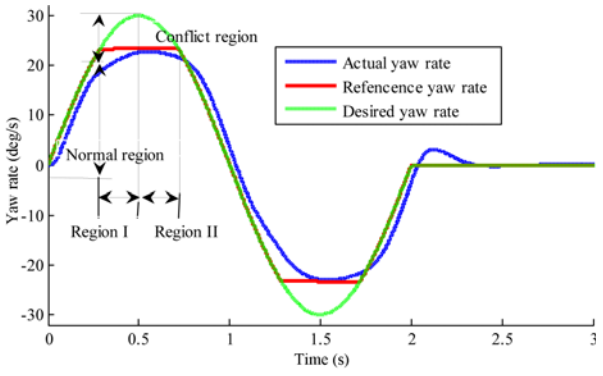

Figure 5. Yaw rate response in sine wave steering maneuver.

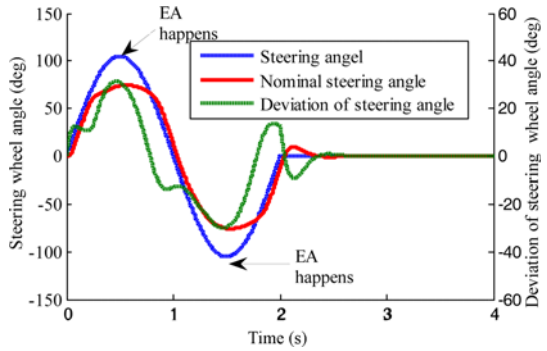

Figure 6. Steering wheel angle information.

$$\delta_n = \frac{1+\frac{m}{l^2}\left(\frac{l_f}{C_r}-\frac{l_r}{C_f}\right)v_x^{\,2}}{v_x/l}\gamma\cdot i_f \tag{7}$$

We use the error between δ_n and δ_{sw} to represent the deviation between the vehicle yaw rate response and the steering wheel angle which shows the driver's intention directly.

$$e_\delta = \delta_{sw} - \delta_n \tag{8}$$

As Figure 6 shows, e_δ reaches maximum value twice at EA situation which means the deviation is largest at the EA stage. The vehicle response cannot satisfy driver's intention at EA situation.

Furthermore, we have conducted simulation in double

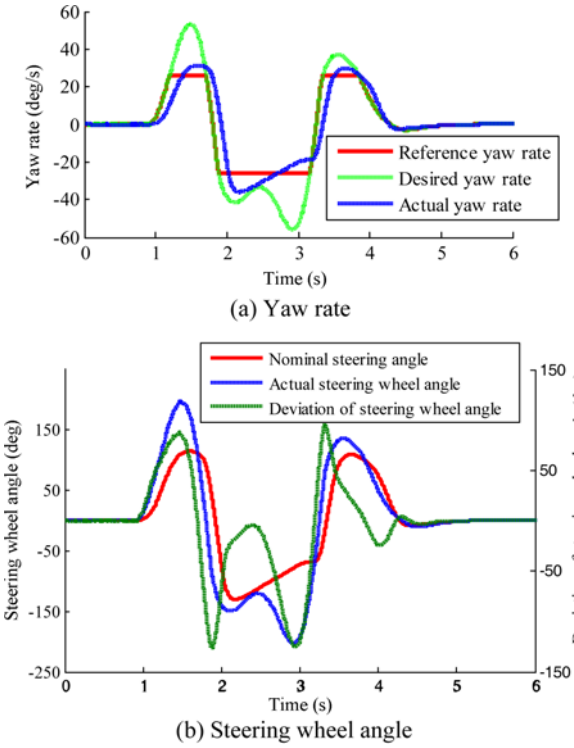

Figure 7. Double lane change maneuver.

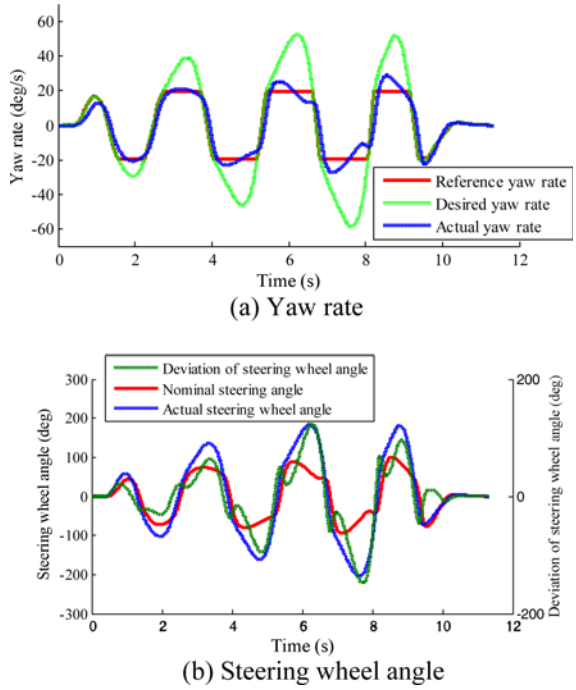

Figure 8. Slalom maneuver.

lane change and slalom maneuvers according to ISO 3888-1:1999(E) and GB/T 6323.1-2014. Figures 7 and 8 depict the simulation results. In double lane change maneuver, the longitudinal velocity is 60 km/h and in slalom maneuver, the longitudinal velocity is 80 km/h. The maximum road friction coefficient is 0.8.

Figures 7 and 8 show that every EA time when the driver decreases the steering wheel angle to the opposite direction fast, the error e_δ gets to its peak value which proves again the vehicle response cannot satisfy driver's intention at EA situation. The error e_δ is significant variable to reflect the deviation between the vehicle yaw rate response and the driver's intention. Therefore we will use this variable to modify the reference model in order to reflect and satisfy the driver's intention.

3. ESC REFERENCE MODEL MODIFICATION STRATEGY

Figure 9 shows the holistic structure of the close-loop vehicle dynamics control system. The reference model modification strategy is given by the green and brown blocks in the Figure 9. The driver's EA intention could be abstracted from the steering wheel angle and its speed. In EA situation, the steering wheel angle signal submits to $\delta_{sw}\cdot\dot{\delta}_{sw}<0$, and the deviation e_δ could be used to reflect the driver's intention. The *SOI* is involved to modify the reference yaw rate.

3.1. Driver's EA Intention Recognition Module

The schematic diagram in Figure 10 shows the driver's EA intention recognition methodology. The sign of $\delta_{sw}\cdot\dot{\delta}_{sw}$ is used to judge if the driver is emergently aligning since the sign of $\delta_{sw}\cdot\dot{\delta}_{sw}$ would be negtive in EA situation. Some complementary rules in the following are used to avoid misrecognizing the EA intention.

(1) $|\delta_{sw}|>\delta_{sw\_lower\ limit}$ and $|\dot{\delta}_{sw}|>\dot{\delta}_{sw\_lower\ limit}$ are needed and have to last for a while longer than T_{act} to prevent the frequent misrecognition when vehicle starts or stops and the driver has to modify the steering wheel slightly and fluently.

(2) If one of the conditions containing $\delta_{sw}\cdot\dot{\delta}_{sw}\geq 0$, $|\delta_{sw}|\leq\delta_{sw\_lower\ limit}$, and $|\dot{\delta}_{sw}|<\dot{\delta}_{sw\_lower\ limit}$ is satisfied and last for a while ($>T_{exit}$), the recognition module turns off.

When the flag in Figure 10 equals 1, the recognition module is activated. When the flag in Figure 10 equals 0, the recognition module is turned off.

Since the vehicle is not equipped with steering wheel angle speed sensor, before calculate the derivative of the steering wheel angle, a recursive average filter as shown in Equation (8) is used to process the steering wheel angle signal.

$$\delta_i=\begin{cases}\delta_i & i<n\\ \dfrac{\sum_{i-n+1}^{i}\delta_j}{n} & i\geq n\end{cases} \tag{9}$$

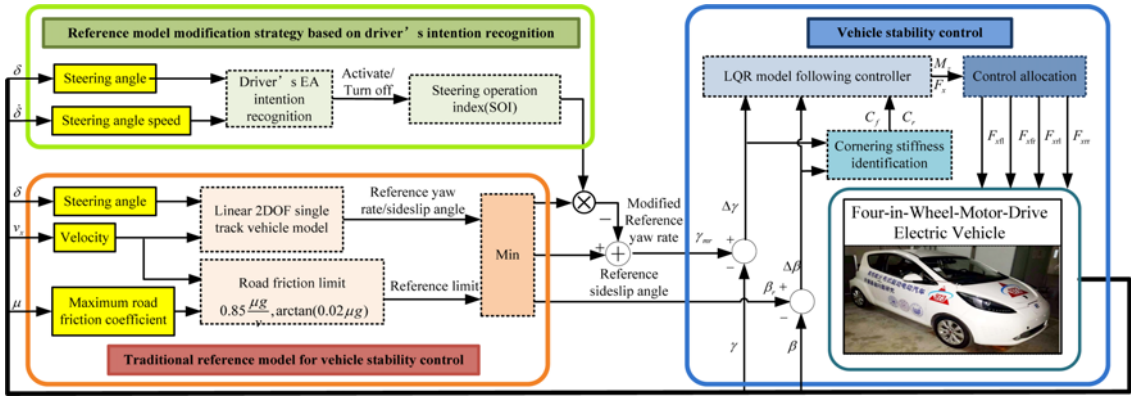

Figure 9. Reference model modification strategy diagram.

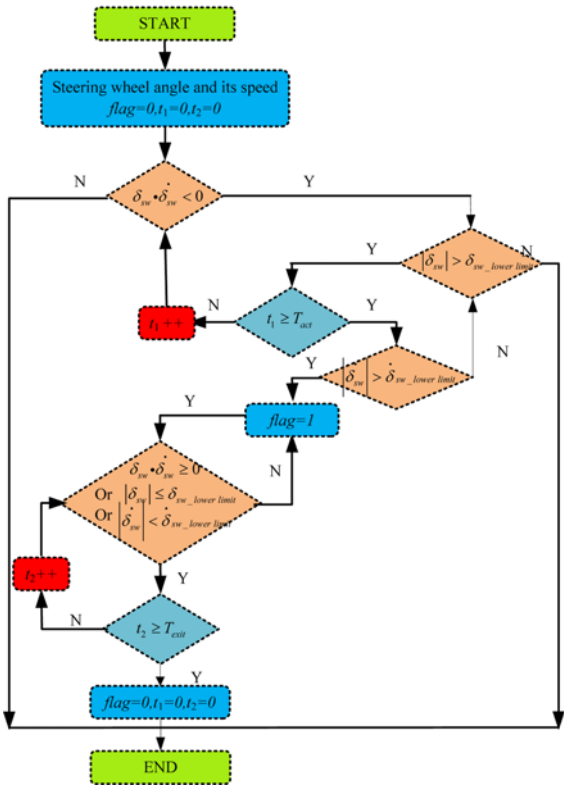

Figure 10. Driver's EA intention recognition module schematic diagram.

$$\dot{\delta}_{\mathrm{i}}=\frac{\Delta\delta_{\mathrm{i}}}{\Delta t} \tag{10}$$

3.2. Reference Model Modification Method

As is mentioned above, the SOI is used to modify the reference model in EA situation. SOI is a function about the deviation e_δ. The function should have the following characteristics:

(1) When the deviation e_δ appears at the very start, the derivative of SOI should be large enough to guarantee that the reference yaw rate could be modified sharply to create a large yaw rate tracking error. When the deviation e_δ increases to a certain value gradually, the derivative of SOI is supposed to decrease gradually until the reference yaw rate is modified to zero;

(2) SOI needs to range from 0 to 1.

Based on the requirement above SOI is defined as Equation (11).

$$SOI=\begin{cases}\sin\dfrac{\pi}{200}\left|\delta_{\mathrm{sw}}-\delta_{\mathrm{n}}\right|, & \left|\delta_{\mathrm{sw}}-\delta_{\mathrm{n}}\right|<100^{\circ}\\ 1, & \left|\delta_{\mathrm{sw}}-\delta_{\mathrm{n}}\right|\geq 100^{\circ}\end{cases} \tag{11}$$

Since only the recognition module is activated (flag = 1), the reference yaw rate starts to be modified. Therefore, the modified reference yaw rate is shown in Equation (12).

$$\gamma_{\mathrm{mr}}=(1-SOI\cdot\mathrm{flag})\cdot\gamma_{\mathrm{r}} \tag{12}$$

4. ESC CONTROLLER

In order to validate the effectiveness of the modified reference model above, a LQR with cornering stiffness identification model following controller (Xiong *et al*., 2012) in our previous work is used for vehicle stability control as shown in the blue block of Figure 9.

4.1. Reference Model

The reference model is used to calculate the reference yaw rate and reference sideslip angle for the MFC to track. γ_{mr} is derived from Equation (11). The rule of determination of reference sideslip angle is shown in Equation (13): When actual sideslip angle β is less than a threshold value $\beta_{\text{lower limit}}$, the reference sideslip angle β_{r} equals β. When β is more than $\beta_{\text{upper limit}}$, it indicates the vehicle is in an unsteady state or about to lose stability, and β_{r} is set to zero. Else, the value of β_{r} is determined according to their linear relationship (Teng *et al*., 2015).

$$\beta_{\mathrm{r}}=\begin{cases}\beta,\ if\ \beta\leq\beta_{0}\\ \dfrac{\beta_{\text{lower limit}}(\beta_{\text{upper limit}}-|\beta|)}{\beta_{\text{upper limit}}-\beta_{\text{lower limit}}}\cdot\mathrm{sgn}(\beta),\ if\ \beta_{\text{lower limit}}<\beta<\beta_{\text{upper limit}}\\ 0,\ if\ \beta\geq\beta_{\text{upper limit}}\end{cases} \tag{13}$$

In this paper, the value of $\beta_{\text{lower limit}}$ is 2°. Referring to (Rajamani, 2005), an empirical equation of for $\beta_{\text{upper limit}}$ is

$$\beta_{\text{upper limit}}=\tan^{-1}(0.02\mu\,\mathrm{g}) \tag{14}$$

4.2. Model Following Controller Based on Tire Cornering Stiffness Identification

The dynamics of the linear 2DOF single track vehicle model is illustrated by Equation (15).

$$\begin{pmatrix}\dot{\beta}\\ \dot{\gamma}\end{pmatrix}=\underbrace{\begin{bmatrix}a_{11} & a_{12}\\ a_{21} & a_{22}\end{bmatrix}}_{A}\begin{pmatrix}\beta\\ \gamma\end{pmatrix}+\underbrace{\begin{bmatrix}b_{11} & b_{12}\\ b_{21} & b_{22}\end{bmatrix}}_{B}\begin{pmatrix}\delta_{\mathrm{f}}\\ M_{\mathrm{z}}\end{pmatrix} \tag{15}$$

Where

$$A=\begin{bmatrix}-\dfrac{C_{\mathrm{f}}+C_{\mathrm{r}}}{mv_{\mathrm{x}}} & -1-\dfrac{l_{\mathrm{f}}C_{\mathrm{f}}-l_{\mathrm{f}}C_{\mathrm{r}}}{mv_{\mathrm{x}}^{2}}\\ -\dfrac{l_{\mathrm{f}}C_{\mathrm{f}}-l_{\mathrm{f}}C_{\mathrm{r}}}{J_{\mathrm{z}}} & -\dfrac{l_{\mathrm{f}}^{2}C_{\mathrm{f}}+l_{\mathrm{r}}^{2}C_{\mathrm{r}}}{J_{\mathrm{z}}v_{\mathrm{x}}}\end{bmatrix},$$

$$B=\begin{bmatrix}\dfrac{C_{\mathrm{f}}}{mv_{\mathrm{x}}} & 0\\ \dfrac{l_{\mathrm{f}}C_{\mathrm{f}}}{J_{\mathrm{z}}} & \dfrac{1}{J_{\mathrm{z}}}\end{bmatrix},\ \text{and}\ x=\begin{bmatrix}\beta & \gamma\end{bmatrix}^{\mathrm{T}}.$$

According to Xiong *et al*. (2012), cornering stiffness of the tyre is an important parameter for the controller. It fluctuates under varying road conditions, or when the vehicle is under critical condition, which affects the effect of the vehicle stability control. Therefore, the tyre cornering stiffness is estimated in real time in order to improve the control effects.

Equation (15) can be written as

$$y(t) = \phi^{\mathrm{T}}(t) \cdot \theta \tag{16}$$

where $y = \begin{bmatrix} ma_{\mathrm{y}} \\ J_{\mathrm{Z}}\dot{\gamma} - M_{\mathrm{z}} \end{bmatrix}$ is the observation vector,

$\phi = [\phi_1,\ \phi_2] = \begin{bmatrix} \beta + \frac{l_{\mathrm{f}}\gamma}{v_{\mathrm{x}}} - \delta_{\mathrm{f}} & (\beta + \frac{l_{\mathrm{f}}\gamma}{v_{\mathrm{x}}} - \delta_{\mathrm{f}})l_{\mathrm{f}} \\ \beta - \frac{l_{\mathrm{r}}\gamma}{v_{\mathrm{x}}} & -(\beta - \frac{l_{\mathrm{r}}\gamma}{v_{\mathrm{x}}})l_{\mathrm{r}} \end{bmatrix}$ is the measured vector and $\theta = [\theta_1\ \ \theta_2]^{\mathrm{T}} = [C_{\mathrm{f}}\ C_{\mathrm{r}}]^{\mathrm{T}}$ is the estimated vector.

Based on the above model, the front and rear cornering stiffness C_{f}, C_{r} can be estimated by recursive least square with forgetting factors algorithm as follows:

$$\begin{cases} L_1(k) = P_1(k-1)\phi_1(k)(\lambda_1 + \phi_1^{\mathrm{T}}(k)P_1(k-1)\phi_1(k))^{-1} \\ P_1(k) = (I - L_1(k)\phi_1^{\mathrm{T}}(k))P_1(k-1)\dfrac{1}{\lambda_1} \end{cases} \tag{17}$$

$$\begin{cases} L_2(k) = P_2(k-1)\phi_2(k)(\lambda_2 + \phi_2^{\mathrm{T}}(k)P_2(k-1)\phi_2(k))^{-1} \\ P_2(k) = (I - L_2(k)\phi_2^{\mathrm{T}}(k))P_2(k-1)\dfrac{1}{\lambda_2} \end{cases} \tag{18}$$

$$\begin{bmatrix} \hat{\theta}_1(k) \\ \hat{\theta}_2(k) \end{bmatrix} = \begin{bmatrix} 1 & L_1(k)\phi_2(k) \\ L_2(k)\phi_1(k) & 1 \end{bmatrix}^{-1} \cdot \begin{bmatrix} \hat{\theta}_1(k-1) + L_1(k)(y(k) - \phi_1(k)\hat{\theta}_1(k-1)) \\ \hat{\theta}_2(k-1) + L_2(k)(y(k) - \phi_2(k)\hat{\theta}_2(k-1)) \end{bmatrix} \tag{19}$$

where λ_1 and λ_2 are needed to be tuned offline.

Adaptive control algorithm based on tyre cornering stiffness adaption with Linear Quadratic Regulator theory is adopted and the control structure is shown in Figure 9.

It is assumed that the state equation of reference model can be expressed as

$$\dot{x}_{\mathrm{d}} = A_{\mathrm{d}}x_{\mathrm{d}} + B_{\mathrm{d}}\delta_{\mathrm{f}} \tag{20}$$

And the control tracking error is

$$e = x - x_{\mathrm{d}} \tag{21}$$

Substitute Equations (15) and (20) into Equation (21), then Equation (22) is obtained.

$$\dot{e} = A_{\mathrm{x}}e + B_{\mathrm{M}}u_{\mathrm{M}} + (A_{\mathrm{x}} - A_{\mathrm{d}})x_{\mathrm{d}} + (B_{\delta} - B_{\mathrm{d}})\delta_{\mathrm{f}} \tag{22}$$

The last two terms of the above formula are regarded as disturbance. An integral control method is adopted to offset the influence caused by constant disturbance (Xiong *et al*., 2010). However, it can be found that the two disturbance terms in Equation (22) always change at random and cannot be regarded as constant disturbance. Thus, the influence caused by them cannot be eliminated using the integral control method. Moreover, integral control may cause control delay and bring adverse influence on vehicle control. Therefore, the last two terms in Equation (22) of LQR are always neglected in the field of vehicle stability control (Li *et al*., 2013a; Ding and Guo, 2010). The control law is designed based on standard LQR and optimal objective equation is defined as D

$$\min J = \int_0^{\infty} (e^{\mathrm{T}}Qe + u_{\mathrm{M}}{}^{\mathrm{T}}Ru_{\mathrm{M}}) \tag{23}$$

According to LQR theory, the optimal required yaw moment is defined as

$$u_{\mathrm{M}} = -K_{\mathrm{M}} \cdot e \tag{24}$$

Where the feedback coefficient K_{M} is defined as

$$K_{\mathrm{M}} = \begin{bmatrix} k_{\beta} & k_{\gamma} \end{bmatrix} = R^{-1}B_{\mathrm{M}}{}^{\mathrm{T}}P \tag{25}$$

And P can be achieved by solving the Riccati equation

$$PA_{\mathrm{x}} + A_{\mathrm{x}}{}^{\mathrm{T}}P - PB_{\mathrm{M}}R^{-1}B_{\mathrm{M}}{}^{\mathrm{T}}P + Q = 0 \tag{26}$$

Because the solution of Riccati equation is complex, feedback gains k_{β} and k_{γ} with respect to different cornering stiffness C_{f}, C_{r} and vehicle speeds v_{x} are calculated offline and listed in lookup table. The direct yaw moment is given by Equation (27).

$$M_{\mathrm{z}} = -k_{\beta}(\beta - \beta_{\mathrm{d}}) - k_{\gamma}(\gamma - \gamma_{\mathrm{d}}) \tag{27}$$

Then the total longitudinal force as well as direct yaw moment generated by tire longitudinal forces can be expressed as:

$$\begin{cases} F_{\mathrm{x}} = F_{\mathrm{xfl}} + F_{\mathrm{xfr}} + F_{\mathrm{xrl}} + F_{\mathrm{xrr}} \\ M_{\mathrm{z}} = \dfrac{b}{2}(-F_{\mathrm{xfl}} + F_{\mathrm{xfr}} - F_{\mathrm{xrl}} + F_{\mathrm{xrr}}) \end{cases} \tag{28}$$

where $F_{\mathrm{xfl}}, F_{\mathrm{xfr}}, F_{\mathrm{xrl}}, F_{\mathrm{xrr}}$ denote the longitudinal forces of each wheel.

Equation (28) can be rewritten as:

$$v = Bu_{\mathrm{c}} \tag{29}$$

Where $v = [F_{\mathrm{x}}\ M_{\mathrm{z}}]^{\mathrm{T}}$, $B = \begin{bmatrix} 1 & 1 & 1 & 1 \\ -\frac{b_{\mathrm{f}}}{2} & \frac{b_{\mathrm{f}}}{2} & -\frac{b_{\mathrm{r}}}{2} & \frac{b_{\mathrm{r}}}{2} \end{bmatrix}$,

$u_{\mathrm{c}} = [F_{\mathrm{xfl}}\ F_{\mathrm{xfr}}\ F_{\mathrm{xrl}}\ F_{\mathrm{xrr}}]^{\mathrm{T}}$

Refer to the previous research, the torque allocation algorithm is designed. Load capacity of in-wheel motors and restraint of road adhesion condition were taken into account. The energy efficiency of motors and the longitudinal forces of each wheel were set up as optimized

targets.

The following quadratic programming equation is obtained (Yang *et al*., 2013):

$$\begin{cases} u_c = \arg\min_{u_c \in \Omega} \left\| W_u u_c \right\|_2 \\ \Omega = \arg\min_{u_c^- \le u_c \le u_c^+} \left\| W_v (B u_c - v) \right\|_2 \end{cases} \tag{30}$$

where $W_u = diag\left[\frac{1}{(\mu F_{zi})^2}\right]$ denotes the weight matrice of control inputs u_c, F_{zi} denotes the vertical load, W_v denotes the weight matrice of forces in v and Ω determines the range domain of u_c.

The solution to such problems is called sequential least square, which needs two steps for the computation, while it is also turned into a weighted least square problem:

$$u_c = \arg\min_{u_c^- \le u_c \le u_c^+} \left(\left\| W_u u_c \right\|_2^2 + \eta \left\| W_v (B u_c - v) \right\|_2^2 \right) \tag{31}$$

In this manner, the computing time could be greatly reduced. The weight factor η is usually set to be large enough in order to minimize the allocation error. Finally, the optimization problem can be solved using active set methods.

5. EXPERIMENTAL TEST

5.1. Test Vehicle

The experimental tests were conducted to validate the effectiveness of the proposed reference model modification strategy. The test vehicle is setup from a SAIC Roewe E50 driven by four motors among which two hub motors are mounted to the rear axle and two motor and gear boxes are mounted to the front axle as shown in Figure 11 (a). The vehicle parameters and main powertrain parameters are shown in Tables 1 and 2 respectively. Figure 11 (b) shows the test system configuration. A MicroAutoBox from dSPACE is used for real time controller and data acquisition. The RT3003 from Oxford Technical Solutions is used to measure longitudinal velocity, yaw rate, sideslip angle and lateral acceleration. Motor torque signal is abtained from the motor controllers. The steering wheel angle signal is measured by the Kistler steering wheel.

(a) Four-in-wheel-motor-drive electric test vehicle

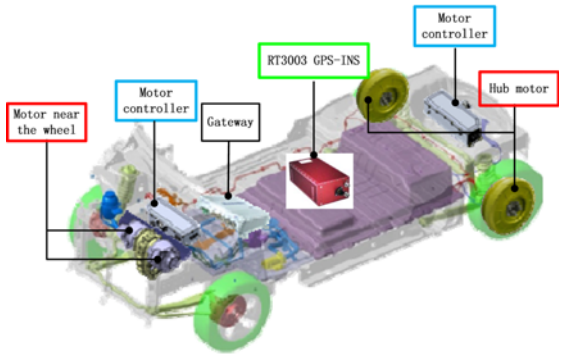

(b) Sensors configuration

Figure 11. FIWMD test EV.

5.2. Experimental Results and Discussion

There are different experimental maneuvers used to evaluate the stability and safety of vehicle, including

Table 2. Motor parameters of test vehicle.

Parameter	Front axle motor	Rear axle motor
Rated power (kW)	15	5
Peak power (kW)	25	7.5
Rated torque (Nm)	35.8	100
Peak torque (Nm)	90	150
Rated speed (rpm)	4000	480
Maximum speed (rpm)	9500	1350
Gear ratio	6.2	1

Table 1. Parameters of the test vehicle.

Parameter	Value	Parameter	Value
Mass (kg)	1358	Yaw moment of inertia (kg·m^2)	1835
Wheel base (m)	2.305	Wheel track (mm)	1325 (Front) / 1390 (Rear)
Distance between COG and front axle (m)	1.117	Distance between COG and front axle (m)	1.188
Height of COG (m)	0.525	Tire rolling radius (m)	0.29
Steering ratio	16.68	Front/Rear axle load	54/46

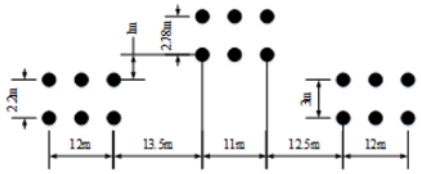

(a) Path setting in double lane change maneuver

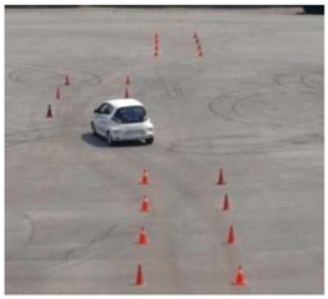

(b) Double lane change maneuver

(c) Path setting in slalom experiment

(d) Slalom maneuver test

Figure 12. Test maneuver.

double lane change, slalom, sine with dwell, and so on. Each maneuver has its own characteristic. Double lane change and slalom tests can reflect the response characteristic of drivers regarding the motion of a vehicle in critical (potentially dangerous) driving situations. Thus, double lane change and slalom maneuvers are adopted in this paper.

The test site is a circle with a radius of 50 m, and the maximum road friction coefficient is about 0.8 when the road is dry. Considering the objective conditions in our school, in accordance with ISO 3888-1:1999(E) and GB/T 6323.1-2014, the schematic diagrams of path setting are depicted as Figure 12. Numerous tests have been done in double lane change and slalom maneuver. The initial entrance velocity is 40 km/h and increases 5 km/h every time. Ten tests need to be done with the same driver at every entrance velocity. The statistics results of pass time

Table 3. Double lane change maneuver.

Velocity	Pass time without control	Pass time with conventional reference model	Pass time with modified reference model
40 km/h	10	10	10
45 km/h	7	9	10
50 km/h	0	3	8
55 km/h	0	0	2

Table 4. Slalom maneuver.

Velocity	Pass time without control	Pass time with conventional reference model	Pass time with modified reference model
40 km/h	6	10	10
45 km/h	0	5	9
50 km/h	0	0	2

are shown in Tables 3 and 4 respectively.

As shown in Tables 3 and 4, in double lane change maneuver, the vehicle without control passes 7 times at 45 km/h initial entrance velocity and it cannot finish the maneuver when the velocity increases more but the vehicle with control can finish the maneuver easily. At 50 km/h, the vehicle with control with the conventional reference model finishes the maneuver only 3 times but the vehicle with control with the modified reference model passes 8 times. At 55 km/h, the vehicle with the modified reference model passes sometimes but the vehicle with the conventional reference model cannot. The same results can also be suggested from Table 4 apparently.

Based on the results in Tables 3 and 4, it can be concluded that the pass velocity, the vehicle stability and safety can be improved with control. When the modified reference model is used the vehicle stability performance can be enhanced further.

In order to compare the results in specific, we take certain test to analyze the vehicle state response in following. The initial velocity is 50 km/h and 45 km/h in double lane change and slalom maneuver respectively.

LQR control with MR means the vehicle is controlled with the modified reference model. LQR control means the vehicle is controlled with the traditional reference model. FL means the front left wheel, FR means the front right wheel, RL means the rear left wheel, and RR means the rear right wheel.

The test results of double lane change and slalom maneuver are presented in Figures 13 and 14. The velocity is shown by Figures 13 (b) and 14 (b). The vehicle without control cannot finish the maneuvers. The sideslip angle would diverge at critical situation in both maneuvers. The red line steering wheel angle signal in Figure 13 (a)

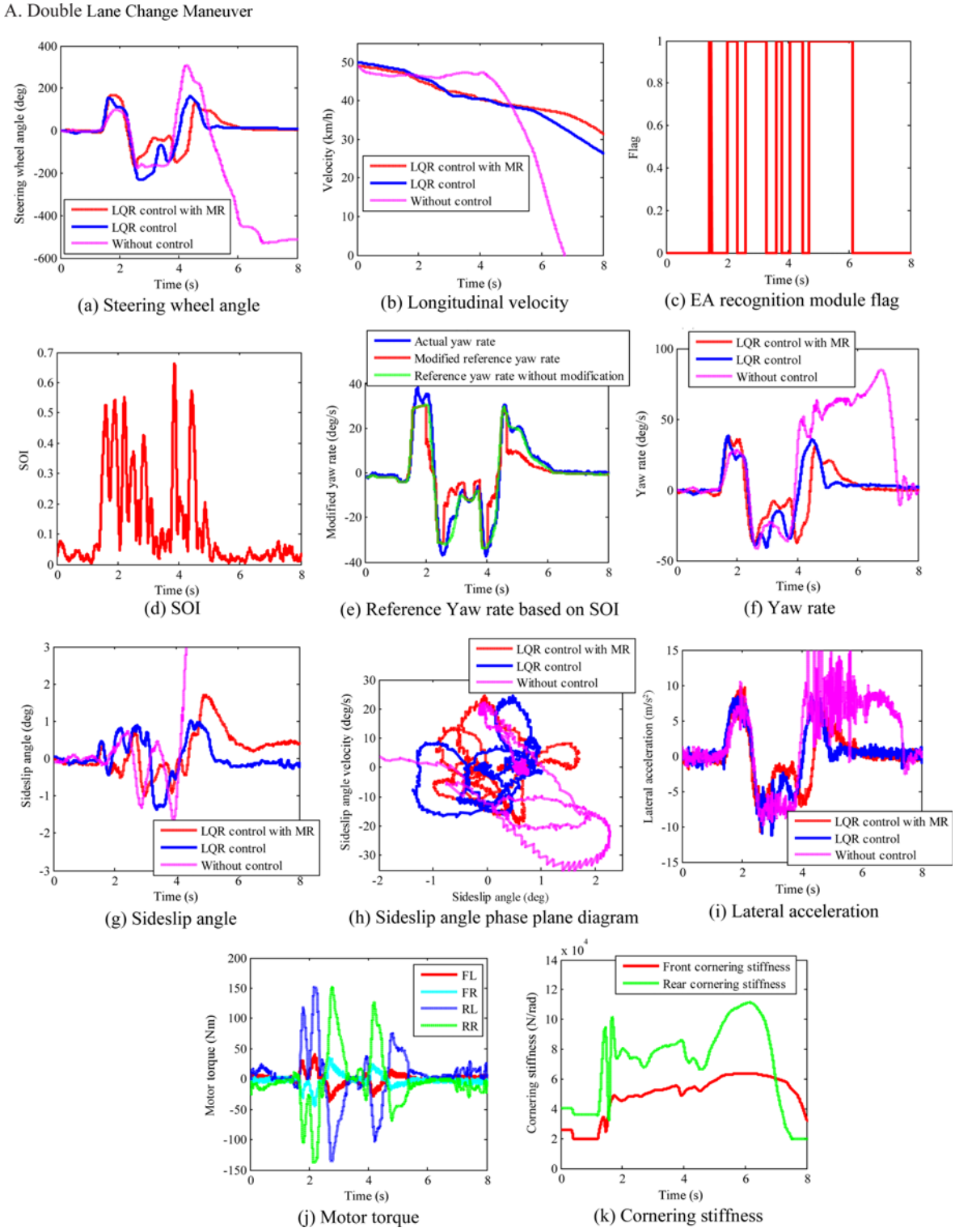

Figure 13. Test results in double lane change maneuver.

suggests that EA (steering wheel angle decreases sharply) happens six times and the recognition module detects them accurately as Figure 13 (c) shows. Compared with double lane change maneuver, in slalom maneuver as shown in Figure 14 (a), there are more EA situation and the recognition module detects them six times as Figure 14 (c) shows. When the flag equals 1, the red lines representing yaw rate in Figures 13 (e) and 14 (e) are pulled down to

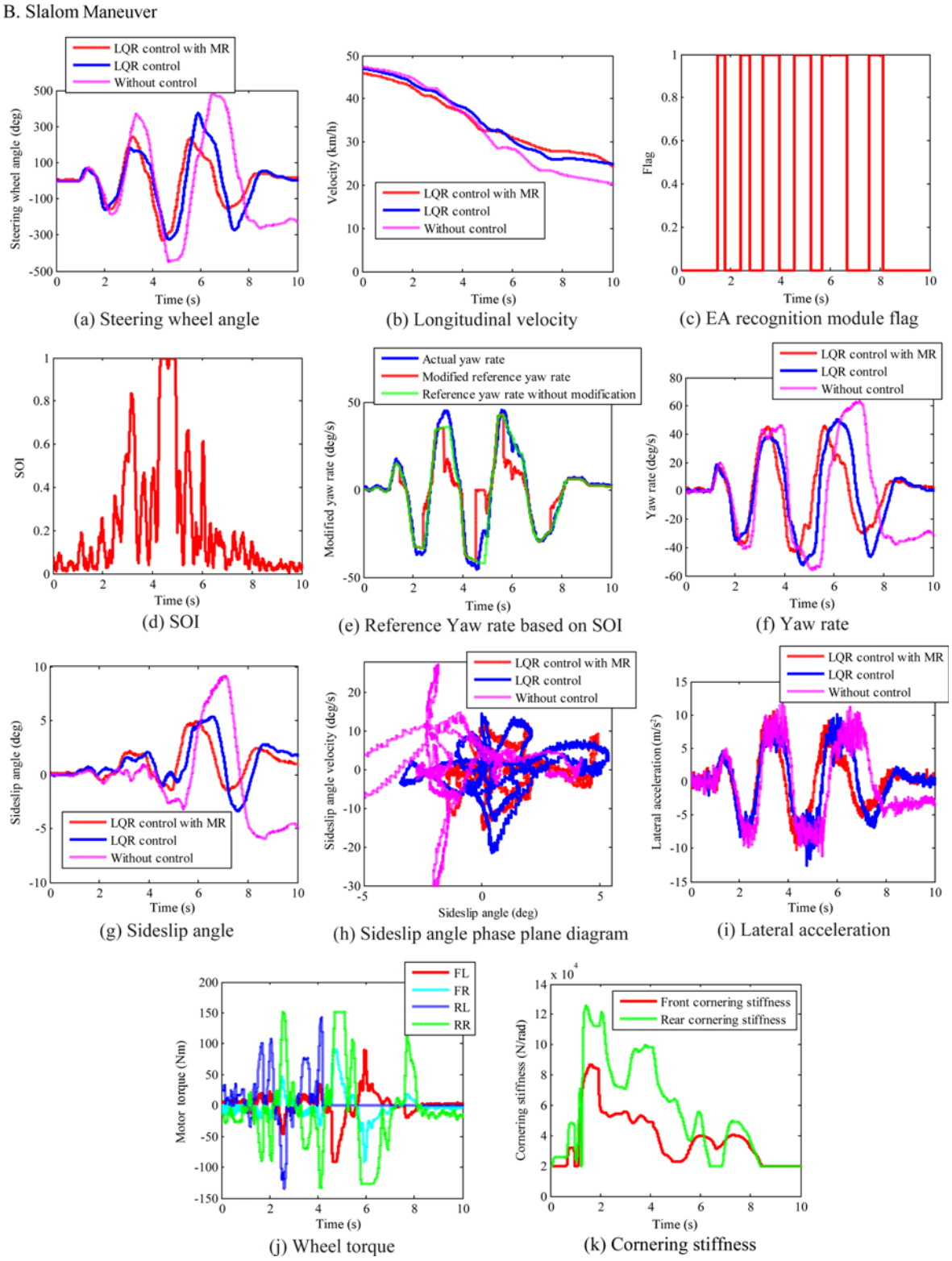

Figure 14. Test results in slalom maneuver.

enlarge the yaw rate tracking error for larger direct yaw moment in EA situation. The details of the *SOI* variation are given by Figures 13 (d) and 14 (d). The direct yaw moment is realized by exerting torques on the four wheels as shown in Figures 13 (j) and 14 (j) to help the driver turn to the opposite direction urgently to fulfill his emergent

alignment intention. Figures 13 (f) and 14 (f) indicate that the red lines which represent the modified yaw rate are much small than the reference yaw rate without modification at EA moment. The actual yaw rate represented by the blue line can follow the driver's intention better in EA situation. The lag of yaw rate response to the steering angle and the peak value of the yaw rate are decreased after using this modification strategy. The driver's burden has been alleviated. The cornering stiffness estimation results are depicted by Figures 13 (k) and 14 (k) which are used to deal with the high nonlinearity of the tires. When the lateral acceleration increases, the cornerring stiffness decreases to involk direct yaw moment to handle the lateral force limitation. From Figures 13 (g), 14 (g), 13 (i), 14 (i), 13 (h) and 14 (h), it is indicated that the peak values of sideslip angel and lateral acceleration have been reduced greatly and the region formed by envelope line of the red line which represents the result with modified reference model is smallest compared with the blue and purple line representing the result without control and with conventional reference model respectively. This means that the vehicle with modified reference model has the more potential to stabilize the vehicle.

6. CONCLUSION

This paper focuses on the vehicle stability control problem under the emergent obstacle avoidance situation. The reference model modification strategy based on the driver's intention is proposed. Using a LQR model following control methodology with cornering stiffness adaption, much simulation and many vehicle tests have been conducted based on the FIWMD EV. The following conclusions can be derived:

(1) Under the emergent obstacle avoidance situation at high velocity, the existing reference model fails to reflect the driver's EA intention. The conflicts between the lag of vehicle response and driver's intention may caused excessive operation such as steering in panic.
(2) The steering wheel angle its speed are involved and combined with steering wheel angle signal to describe the diver's EA intention of steering. The driver's intention recognition module is designed and it is proved that this module can recognize the driver's EA intention accurately and instantly by vehicle test validation.
(3) The reference model modification strategy is proposed based on the *SOI*. With a LQR model following control methodology with cornering stiffness adaption, many vehicle tests in double lane change and slalom maneuver have been conducted. On the one hand, the vehicle stability and safety can be improved. When the modified reference model is used, the vehicle stability performance is enhanced further which means the vehicle with modified reference model has more potential to stabilize the vehicle. On the other hand, the driver's intention can be satisfied better and the driver's burden has been relieved in EA situation.

In this paper, we abstracted driver's EA intention from steering wheel angle and its speed. Steering torque is another important information to describe the driver's demand and intention (Enache *et al*., 2009). Therefore we will fuse them together to develop the EA recognition module better in our future work.

ACKNOWLEDGEMENT−This research is supported by National Science and Techinology Support Program of China (Grant No. 2015BAG17B01), National Key Research and Development Program of China (Grant No. 2016YFB0100901) and National Natural Science Foundation of China (Grant No. U1564207).

REFERENCES

Abe, M. (1999). Vehicle dynamics and control for improving handling and active safety: From four-wheel steering to direct yaw moment control. *Proc. Institution of Mechanical Engineers, Part K: J. Mult-Body Dynamics* **213**, **2**, 87−101.

Abe, M. (2009). *Vehicle Handling Dynamics*. Oxford: Butterworth-Heinemann. Oxford, UK.

Alipour, H. and Sabahi, M. (2015). Lateral stabilization of a four wheel independent drive electric vehicle on slippery roads. *Mechatronics*, **30**, 275−285.

Anton, T., Zanten, V., Erhardt, R., Landesfeind, K. and Pfaff, G. (1998). VDC systems development and perspective. *SAE Paper No*. 980235.

Chen, J., Song, J., Li, L., Ran, X., Jia, G. and Wu, K. (2016). A novel pre-control method of vehicle dynamics stability based on critical stable velocity during transient steering maneuvering. *Chinese J. Mechanical Engineering* **29**, **3**, 475−485.

Ding, N. and Taheri, S. (2010). An adaptive integrated algorithm for active front steering and direct yaw moment control based on direct Lyapunov method. *Vehicle System Dynamics* **48**, **10**, 1193−1213.

Ding, H. and Guo, K. (2010). LQR method for vehicle yaw moment decision in vehicle stability control. *J. Jilin University*, **3**, 597−601.

Emirler, M., Kahraman, K., Senturk, M., Acar, O., Guvenc, B., Guvenc, L. and Efendioglu, B. (2015). Lateral stability control of fully electric vehicles. *Int. J. Automotive Technology* **16**, **2**, 317−328.

Enache, N., Netto, M., Mammar, S. and Lusetti, B. (2009). Driver steering assistance for lane departure avoidance. *Control Engineering Practice* **17**, **6**, 642−651.

Erke, A. (2008). Effects of electronic stability control (ESC) on accidents: A review of empirical evidence. *Accident Analysis and Prevention* **40**, **1**, 167−173.

Geng, C., Mostefai, L., Denaï, M. and Hori, Y. (2009). Direct yaw-moment control of an in-wheel-motored electric vehicle based on body slip angle fuzzy observer. *IEEE Trans. Industrial Electronics* **56**, **5**, 1411−1419.

Gan, Z., Wang, J. and Guo, J. (2014). Multi-control state and switch conditions design for vehicle electric stability program. *J. Mechanical Engineering* **50**, **4**, 107–112.

Lee, J., Choi, J., Yi, K., Shin, M. and Ko, B. (2014). Lane-keeping assistance control algorithm using differential braking to prevent unintended lane departures. *Control Engineering Practice*, **23**, 1–13.

Li, B., Dong, W. and Wang, X. (2013a). Design and simulation of an active vibration isolator based on pneumatic-electromagnetic hybrid driving. *J. Northwestern Polytechnical University* **31**, **6**, 871–877.

Li, L., Jia, G., Chen, J., Zhu, H., Cao, D. and Song, J. (2015). A novel vehicle dynamics stability control algorithm based on the hierarchical strategy with constrain of nonlinear tyre forces. *Vehicle System Dynamics* **53**, **8**, 1093–1116.

Li, L., Jia, G., Song, J. and Ran, X. (2013b). Progress on vehicle dynamics stability control system. *J. Mechanical Engineering* **49**, **24**, 95–107.

Peng, H. and Hori, Y. (2006). Optimum traction force distribution for stability improvement of 4WD EV in critical driving condition. *Proc. 9th IEEE Int. Workshop on Advanced Motion Control*, 206–211.

Rajamani, R. (2005). *Vehicle Dynamics and Control*. Springer. Minneapolis, Minnesota, USA.

Raksincharoensak, P., Mizushima, T. and Nagai, M. (2009). Direct yaw moment control system based on driver behavior recognition. *Vehicle System Dynamics* **46**, **Supplement 1**, 911–921.

Shen, Y., Gao, Y. and Xu, T. (2016). Multi-axle vehicle dynamics stability control algorithm with all independent drive wheel. *Int. J. Automotive Technology* **17**, **5**, 795–805.

Shibahata, Y., Shimada, K. and Tomari, T. (1993). Improvement of vehicle maneuverability by direct yaw moment control. *Vehicle System Dynamics* **22**, **5**, 465–481.

Shino, M. and Nagai, M. (2001). Yaw-moment control of electric vehicle for improving handling and stability. *JSAE Review* **22**, **4**, 473–480.

Shino, M. and Nagai, M. (2003). Independent wheel torque control of small-scale electric vehicle for handling and stability improvement. *JSAE Review* **24**, **4**, 449–456.

Tahami, F., Kazemi, R., Farhanghi, S. and Samadi, B. (2002). Fuzzy based stability enhancement system for a four-motor-wheel electric vehicle. *SAE Paper No*. 2002-01-1588.

Teng, G., Xiong, L., Leng, B. and Hu, S. (2015). A novel reference model for vehicle dynamics control. *IAVSD*, Graz, Austria.

Xia, X., Xiong, L., Hou, Y., Teng, G. and Yu, Z. (2016). A novel reference model for vehicle stability control based on yaw rate prediction and driver's intention. *Proc. FISITA 2016*, BEXCO, Korea.

Xiong, L., Teng, G., Yu, Z., Zhang, W. and Feng, Y. (2016). Novel stability control strategy for distributed drive electric vehicle based on driver operation intention. *Int. J. Automotive Technology* **17**, **4**, 651–663.

Xiong, L., Chen, C. and Feng, Y. (2014). Modeling of distributed drive electric vehicle based on co-simulation of Carsim/Simulink. *J. System Simulation* **26**, **5**, 1143–1148.

Xiong, L., Yu, Z., Jiang, W. and Jiang, Z. (2010). Research on vehicle stability control of 4WD electric vehicle based on longitudinal force control allocation. *J. Tongji University*, **3**, 417–421.

Xiong, L., Yu, Z., Wang, Y., Chen, Y. and Meng, Y. (2012). Vehicle dynamics control of four in-wheel motor drive electric vehicle using gain scheduling based on tire cornering stiffness estimation. *Vehicle System Dynamics* **50**, **6**, 831–846.

Yang, C. (2011). *Research on 4WD EV Stability Control*. M. S. Thesis. Tongji University. Shanghai, China.

Yang, P., Xiong, L., Zhang, K. and Yu, Z. (2013). Stability control strategy design and experiment of distributed electric drive vehicle. *J. Mechanical Engineering* **49**, **24**, 128–134.

Yang, X., Wang, Z. and Peng, W. (2009). Coordinated control of AFS and DYC for vehicle handling and stability based on optimal guaranteed cost theory. *Vehicle System Dynamics* **47**, **1**, 57–79.

Yu, Z., Leng, B., Xiong, L., Feng, Y. and Xia, X. (2015). Vehicle stability self-tuning control strategy based on joint criterion. *Proc. 24th Symp. Int. Association for Vehicle System Dynamics*, 481–489.

Yu, Z., Gao, X. and Zhang, L. (2006). A study on coordination of direct yaw moment control and variable wheel slip control for vehicle stability. *Automotive Engineering* **28**, **9**, 844–848.

Yu, Z., Feng, Y. and Xiong, L. (2013). Review on vehicle dynamics control of distributed drive electric vehicle. *J. Mechanical Engineering* **49**, **8**, 105–114.

Zanten, V. (2000). Bosch ESP systems: 5 years of experience. *SAE Paper No*. 2000-01-1633.